TEM-EELS study of low-friction superlattice TiAlN/VN coating: the wear mechanisms

LUO, Q. <http://orcid.org/0000-0003-4102-2129>, ZHOU, Z., RAINFORTH, W. M. and HOVSEPIAN, P. E. <http://orcid.org/0000-0002-1047-0407>

Published version

LUO, Q., ZHOU, Z., RAINFORTH, W. M. and HOVSEPIAN, P. E. (2006). TEM-EELS study of low-friction superlattice TiAlN/VN coating: the wear mechanisms. Tribology Letters, 24 (2), 171-178.

TEM-EELS study of low-friction superlattice TiAlN/VN coating: The wear mechanisms

Q. Luo[a]*, Z. Zhou[b], W. M. Rainforth[b], P.Eh. Hovsepian[a]

[a] Materials Research Institute, Sheffield Hallam University, Sheffield, S1 1WB, UK.
[b] Department of Engineering Materials, University of Sheffield, S1 3JD, UK

Abstract: A 20–50 nm thick tribofilm was generated on the worn surface of a multilayer coating TiAlN/VN after dry sliding test against an alumina counterpart. The tribofilm was characterized by applying analytical transmission electron microscopy techniques with emphasis on detailed electron energy loss spectrometry and energy loss near edge structure analysis. Pronounced oxygen in the tribofilm indicated a predominant tribo-oxidation wear. Structural changes in the inner-shell ionization edges of N, Ti and V suggested decomposition of nitride fragments.

Key Words: TiAlN/VN; Tribofilm; Transmission Electron Microscopy (TEM); Electron Energy Loss Spectrometry (EELS); Wear Mechanisms

1. INTRODUCTION

Tribofilms have been frequently found on the sliding worn surfaces of many ceramics, metals and wearresistant coatings [1–5]. A tribofilm adhered to the base material leads to a three-body sliding system and consequently has significant influence on the friction and wear behaviour depending on the chemical composition and structure of the film. This may include, for example, the reduced mechanical wear of hard surfaces by re-distribution of contact stresses, a transition from severe to mild wear after the formation of oxide films on metallic worn surfaces, and self-lubrication property in case of a low shear strength tribofilm. On the other hand, the characterization and analysis of tribofilm provides fingerprint information for the origin of wear product and its interactions with environment species. In recent years, many sophisticated surface analysis techniques have been applied in worn surface and tribofilm analysis [1–10]. Among these techniques, transmission electron microscopy (TEM) is known to have the best spatial resolution for imaging and the multiple capabilities of chemical and structural analyses. In particular, the complementary techniques of energy dispersive X-ray spectrometry (EDX) and electron energy loss spectrometry (EELS) provide opportunity of both qualitative and quantitative chemical analyses to nanometer scale [11,12]. Despite these advantages, however, only limited literatures of TEM based wear mechanism study are available. This is partially due to the challenge in cross-section TEM thin foil preparation.

In this paper, we report the latest progress in the wear mechanism study by employing the state-of-art analytical TEM techniques. The research was performed on a recently developed low-friction and wear-resistant hard coating, namely TiAlN/VN, being grown by combined cathodic arc and unbalanced magnetron sputter deposition. The TiAlN/VN is a multilayer nitride coating having nanometer-scale TiAlN and VN bi-layers, a NaCl-type cubic structure, and polycrystalline columnar morphology [13,14]. Its outstanding tribological properties, as compared to other hard nitrides in the TiN and TiAlN family, are the combined low dry sliding friction coefficient (μ= 0.4–0.6) and extremely low wear rate in a scale of $10^{-17}m^3N^{-1}m^{-1}$ [15,16]. This has led to successful applications in cutting tools in dry milling wrought and cast aluminium alloys [17, 18].

Up to date, a series of experiments have been conducted to investigate the friction and wear mechanisms of the TiAlN/VN coating. By using Raman spectroscopy, V_2O_5-type structure was detected in the wear debris of TiAlN/VN [19], indicative of a major wear mechanism of tribo-oxidation. Meanwhile, it was found in a series of iso-thermal annealing tests that TiAlN/VN coatings for a range of chemical compositions oxidize at temperatures between 500 and 700 ^{0}C, which is obviously lower than the onset oxidation temperature of TiAlN (700–800 ^{0}C). The oxidation led to the formation of a number of oxides, including V_2O_5 and other types like $AlVO_4$, TiO_2 and Al_2TiO_5 [15, 20, 21]. Note that the oxide V_2O_5 has an orthorhombic layer structure with layers stacking along the c-axis [22, 23]. The week interlayer V–O interaction makes easy the cleavage and shear deformation of the structure and therefore brings in some solid-lubricating property. It was therefore speculated that the V2O5 oxide in the wear product, if adhered on the worn surface, is responsible for the low

friction coefficient [15, 24]. However, more details of the wear mechanisms of the TiAlN/VN were not clear.

Recently, cross-sectional TEM observation of tested TiAlN/VN samples revealed the formation of a tribofilm adhered on the worn surface. The first results have been published in [25] and were compared to the tribofilm and worn surface features of a high-friction hard coating TiAlCrYN [26–28]. In brief, the tribofilm observed was amorphous, homogeneous and 20–50 nm thick. It kept a clear boundary to the adjacent nitride and contained substantial amount of oxygen in a multicomponent V–Ti–Al–O composition. TEM-EDX detection of oxygen in the tribofilm as well as in the wear debris confirmed tribo-oxidation as a major wear mechanism. However, several important details still remained unclear concerning the mechanisms of tribo-oxidation wear and mechanical wear. First, it was not clear whether any trace of nitrogen still remained in the tribofilm, which relates to the possible occurrence of mechanical wear of the nitride. Secondly, it was not clear how the nitride was transformed to oxide. Thirdly, nothing was known although a clear boundary was found between the tribofilm and the base TiAlN/VN structure, no evidence could be provided by the TEM-EDX for the occurrence of inward diffusion of oxygen. Thus it was not clear how the TiAlN/VN was oxidized in the sliding contact. These problems are due to the instrumental limitations of EDX analysis, i.e. the low energy resolution (approximately 10 eV for 1024 channels covering a period of 10 keV) unable to resolve the energy position of characteristic X-rays N-K_α, O-Kα, Ti-Lα and V-Lα, and the pronounced mass absorption effect for the above low-energy signals. Therefore further chemical and structural characterizations are demanded to find more evidences explaining the wear mechanisms. Considering this issue, this paper is focused on detailed comparative study of the EELS data acquired from the tribofilm, the loose wear debris and the TiAlN/VN nitride. It is also extended to the energy loss near edge structure (ELNES) analysis for more precise structural and bonding investigation.

2. EXPERIMENTAL METHODS

2.1. Coating preparation and wear test

The TiAlN/VN multilayer coating was grown on polished steel coupons by using a four-cathode (two $Ti_{0.5}Al_{0.5}$ and two pure vanadium at purity of 99.98 at.%) PVD coater operating in unbalanced magnetron sputtering mode, under a substrate bias voltage -75V, in a reactive atmosphere of Ar + N2 at temperature 450 ^{0}C. Prior to the deposition of TiAlN/VN, one of the V cathodes was operated in arc mode for metal-ion etching of the substrate surface followed by sputter deposition of a VN base layer. Detailed deposition parameters have been reported in previous publications [13, 14].

A CSM pin-on-disc tribometer was employed to perform the wear test at the following conditions: a 6 mm in diameter Al_2O_3 ball counterpart, normal load 5 N, linear sliding speed 0.1 m s^{-1}, total sliding durations of 200,000 laps leading to a sliding distance of 12.6 km, room temperature 20–30 ^{0}C, and dry sliding at relative humidity 30–40%. Detailed mechanical and tribological evaluation has been published elsewhere [16].

2.2. TEM sample preparation, TEM, EDX and EELS analyses

A longitudinal cross-section sample containing the worn surface was sectioned using a high-speed SiC disc saw, which was then thinned following conventional metallographic grinding and polishing procedures to a thickness of 20–50 μm. Final thinning to electron transparency was undertaken on a two-cathode Gatan precision ion polish system by argon ion beam milling. Detailed description of the sample preparation method can be found in literatures [25, 27, 28]. In addition, wear particles generated during the wear tests were collected on a 200-mesh carbon-film copper grid for direct analysis on TEM.

Conventional TEM characterization and EDX analyses were performed on a Philips STEM-CM20 instrument with a LaB_6 filament operating at 200 kV and an attached EDX system. The EDX facility comprises an ultra-thin window X-ray detector and a Link ISIS computer system (The Oxford Instruments plc). EELS analysis was performed in a JEOL 2010F field emission gun TEM operating at 200 kV and equipped with GATAN Imaging Filter (GIF200). The instrument is capable of generating useful analytical probe of 1–2 nm in diameter and provides a routine energy resolution for EELS studies of 1.2 eV, with 0.65 eV possible under ideal conditions. Spectrometer energy dispersion of 0.2–0.3 eV per channel was used with convergence and collection semi-angles of 8.5 and 4.8 mrad respectively. Electron energy loss spectra were acquired in typical areas of tribofilm, TiAlN/VN multilayer, and VN base layer as well as from the loose wear debris. In the current experiment, most of the sample thickness values fell in a range (0.39–1.08)λ where λ is the average mean free path. To ensure acquisition from sample areas thin enough to avoid the need for correction of the spectrum for plural scattering, it was verified that the Plasmon intensity, I_T, was less than one tenth of the zero-loss peak intensity, I_0 [29]. In each acquired spectrum, the plural-scattering induced background intensity was removed by fitting a power law ($I = AE^{-r}$) to the background preceding the edge, extrapolating it under the edge and then subtracting.

3. RESULTS

3.1. Friction and wear properties of TiAlN/VN coating

The average friction coefficient during the sliding wear test of the TiAlN/VN coating was approximately 0.4 and the specific wear rate at the end of the test was measured to be $2.3 \times 10^{-17} m^3 N^{-1} m^{-1}$. The wear track was 0.3 mm wide and approximately 0.5 μm deep as measured by surface profilerometry. Figure 1 is a scanning secondary electron image showing part of the worn surface. The surface was generally smooth but contained longitudinal scratches, which were probably caused by abrasion arising from sliding and or rolling particles trapped within the contact zone. Some loose wear debris was visible on both sides of the wear track. The wear debris exhibited dark contrast as compared to the TiAlN/VN coating. This was attributed to lower counts of secondary electron emission from the wear debris, which was determined to be clusters of amorphous oxide as a result of oxidation wear [25]. Similarly, the worn surface also exhibits a darker contrast compared to the adjacent TiAlN/VN surface, which clearly implies a change in

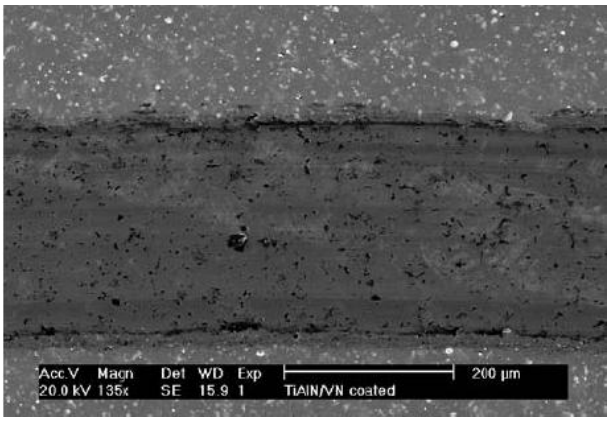

Figure 1. Scanning secondary electron micrograph of the TiAlN/VN worn surface after 200,000 laps dry-sliding against an alumina ball at an applied load 5 N and sliding speed 0.1 m s^{-1}.

surface structure at the worn surface compared to the coating, possibly through the formation of a surface structure with lower electrical conductivity.

3.2. Cross-section TEM and EDX analysis of tribofilm

Observation of the thin film by using cross-sectional TEM is shown in Figure 2, in which a 20–50 nm thick tribofilm can be seen on the top of the TiAlN/VN surface Detailed TEM imaging, electron diffraction and EDX analysis of this region have been described in [25]. It has been found that, the tribofilm is amorphous, porous in nanometer- or atomic-scale, and has a clear boundary to the adjacent TiAlN/VN. The TiAlN/VN at the worn surface cross-section edge shows good structural integrity without any visible crack or deformation, indicating negligible delamination wear or deformation. The prevention of mechanical wear to nanometer scale was in a strike contrast to the behaviour of other high friction nitrides, such as TiAlCrYN where deformation and delamination

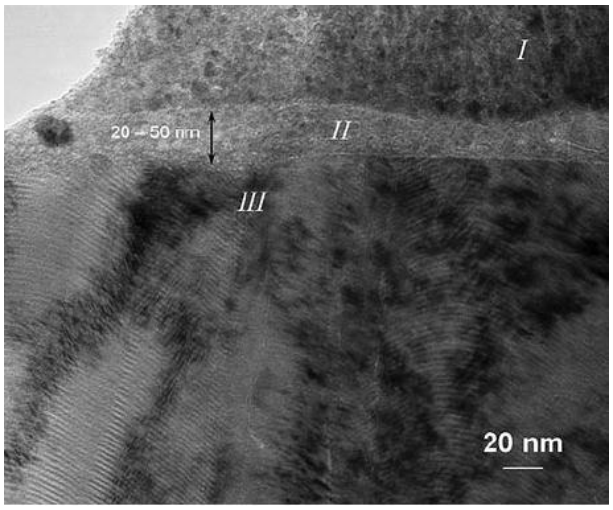

Figure 2. Cross-sectional TEM bright field image of the TiAlN/VN worn surface, showing a 20–50 nm thick tribofilm (region II) on the TiAlN/VN coating (region III). Region I is copper re-deposit formed during the TEM sample preparation (ion-beam thinning).

wear were observed to occur on the worn surface [30].

Figure 3(a) shows an EDX spectrum of the tribofilm as compared to that acquired from the adjacent TiAlN/VN. Both spectra indicate pronounced contents of metals V, Ti and Al. The difference between the two spectra, however, exists in the relative intensity of the low-energy

peaks O-K_α and N-K_α. This is better resolved in Figure 3(b). The tribofilm is obviously rich in oxygen whereas the TiAlN/VN shows a distinct peak N-K_α. The spectra shown in Figure 3 also show the limitation of EDX analysis in the Ti–V–N–O system, i.e. pronounced mass absorption effect and poor energy resolution to distinguish the characteristic X-rays N-K_α, O-K_α, Ti-L_α and V-L_α.

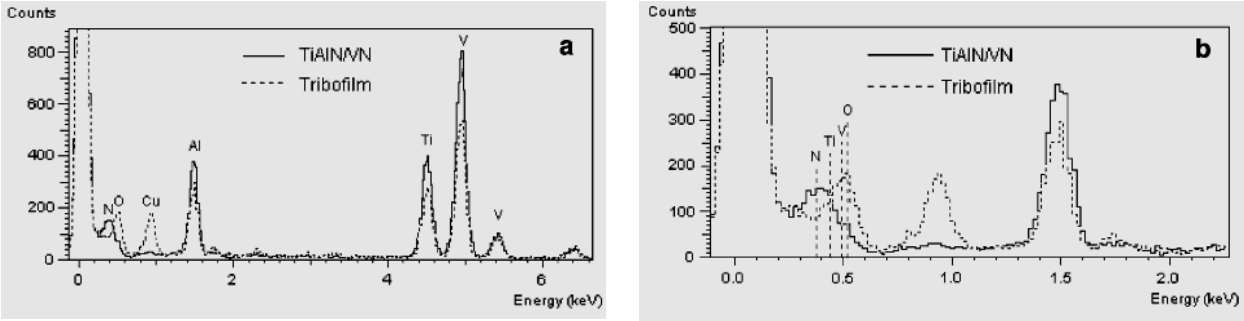

Figure 3. Comparison between the TEM-EDX spectra of the tribofilm and the adjacent TiAlN/VN nitride.

3.3. Transmission electron energy loss spectroscopy of tribofilm, wear debris and the TiAlN/VN coating

In Figure 4, a typical transmission electron energy loss spectrum was acquired in the TiAlN/VN region adjacent to the tribofilm, in the energy loss range between 350 and 650 eV. The EELS spectrum demonstrates its powerful resolution by showing well separated energy loss edges N-K, Ti-$L_{2,3}$ and V-$L_{2,3}$. The spectrum showed a strong N-K edge and the absence of O-K edge. Note that the absence of O-K edge suggests no inward diffusion of oxygen through the tribofilm-nitride boundary. Also according to the cross-sectional imaging, there was no intermediate layer between the tribofilm and the nitride surface for the nitride-oxide transformation. In other words, the oxidation of the TiAlN/VN under the dry sliding was not dominated by a diffusion process. This was confirmed in several EELS spectra acquired in areas adjacent to the tribofilm for a range of local thickness from thin edge (t/λ = 0.31) to the relatively thick area (t/λ = 0.9–1.08), irrespective of changes in background and plasmon peak intensity. Figure 5 is a typical spectrum acquired in the tribofilm region. A strong O-K edge can be seen, which is consistent exactly with the EDX analysis (Figure 3b). Similarly strong O-K edge was also observed in the EELS spectrum of the loose wear debris (supported on carbon grids), Figure 6. Moreover, the EELS spectrum in Figure 5 also shows a

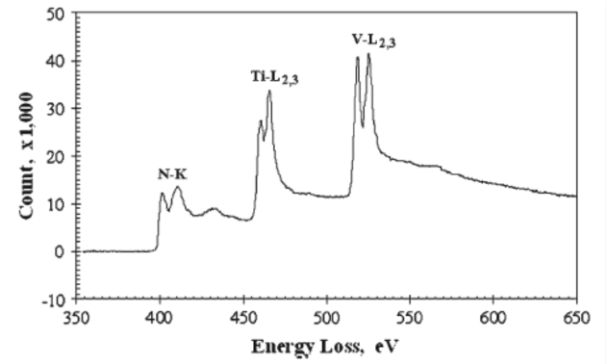

Figure 4. Electron energy loss spectrum of TiAlN/VN. Note the strong N-K edge in addition to the $L_{2,3}$ edges of Ti and V.

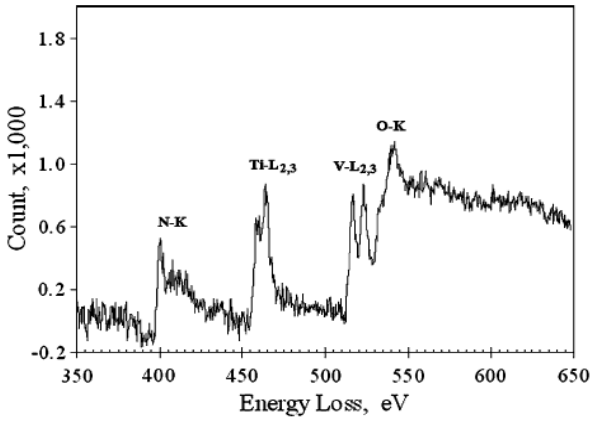

Figure 5. Electron energy loss spectrum of tribofilm acquired for a range of energy loss between 350 and 650 eV at a dispersion of 0.3 eV per pixel. Note the remarkable decrease in the intensity of the N-K edge and the presence of a strong and broad O-K edge, indicating pronounced nitride decomposition and oxidation.

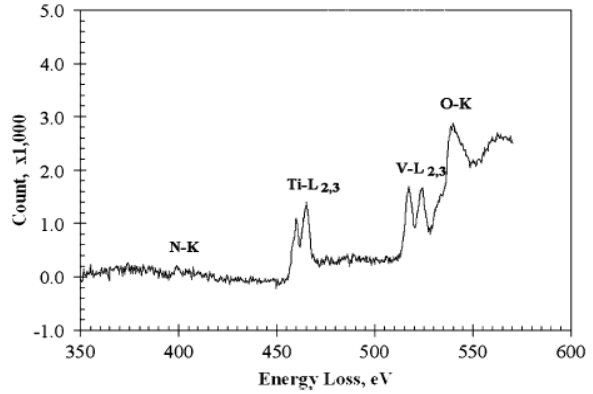

Figure 6. Electron energy loss spectrum of loose wear debris. Note the complete disappearance of the N-K edge and the presence of a strong and broad O-K edge, indicating a predominant wear mechanism of tribo-oxidation.

small but distinct N-K edge, suggesting content of nitride structure in the tribofilm. In the wear debris, however, the N-K edge was hard to see, i.e. being as low as the background noise, indicative of complete oxidation.

The EELS data in Figures 4–6 indicate the different chemical compositions from the coating area, the tribofilm and the loose wear debris. The coating was confirmed to be pure nitride free from oxygen. The transition from the TiAlN/VN coating to the tribofilm appeared to be abrupt, with no intermediate structure observed, Figure 2, indicating no inward diffusion of oxygen into the coating prior to formation of the tribofilm. The tribofilm showed co-existence of oxygen and nitrogen, whereas the nitrogen in the wear debris was completely lost or replaced by oxygen. Obviously tribo-oxidation occurred only or mostly in the volume of tribofilm which was directly exposed to mechanical and chemical attack. Thus, one can speculate progressive replacement of nitrogen by oxygen in the tribofilm during sliding which proceeds together with the structural amorphization. Eventually nitrogen was completely replaced by oxygen when the film was detached as wear debris.

3.4. ELNES analysis of tribofilm, wear debris and the TiAlN/VN coating

Further evidence of the oxidation process has been found by comparing the near-edge structure of N-K edges, i.e. the ELNES feature, between the TiAlN/VN coating and the tribofilm.

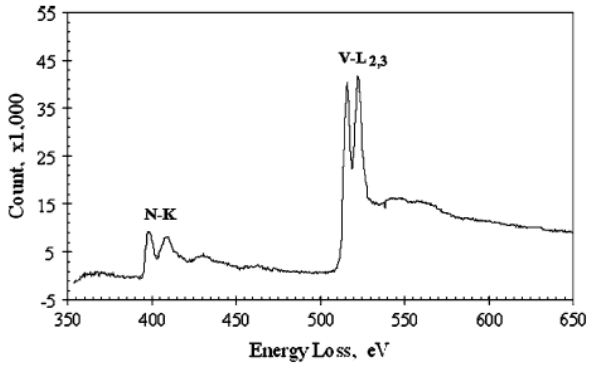

Figure 7. Electron energy loss spectrum acquired from the VN base layer of the coating showing N-K and V-L2,3 edges.

ELNES arises from the energy distribution of the unoccupied electronic states above the Fermi level and is strongly influenced by the local bonding characteristics, coordination and charge distributions of the ionized atoms [31–33]. It can be used as 'fingerprints' to distinguish compounds of similar chemical compositions, such as between VN and V_2N [31,33] and between CrN and Cr_2N [32]. In the current experiments, the TiAlN/VN nitride and the tribofilm exhibited different shapes of the N-K absorption edge from each other. In the TiAlN/VN (Figure 4), an identical ELNES following the ionization threshold of the N-K edge (396 eV) can be seen to have two sharp peaks, at the energy loss of 401.1 and 411.9 eV respectively, as well as a low-intensity and broader peak in the energy loss range between 429.3 and 441.0 eV. Similarly, EELS spectra acquired from the VN base layer also showed an identical double-peak N-K edge, Figure 7. Such N-K ELNES feature is typical for cubic transition metal nitride having stoichiometric nitrogen content [31, 32]. The results are in good agreement to the optimized deposition conditions for reactive deposition of stoichiometric nitride coatings [15, 34]. Unlike the stoichiometric nitrides TiAlN/VN and VN, the tribofilm showed an N-K absorption edge consisting of only one sharp peak followed by a broad low-intensity shoulder. The sharp peak corresponds to the first (i.e. low energy loss) peak in that of the TiAlN/VN, whereas the broad shoulder was a replacement of the second peak. This type of N-K ELNES pattern has been reported in nitrides V_2N and Cr_2N, which contain less nitrogen than the stoichiometric phases. Therefore, the nitride contained in the tribofilm was suspected to have been partially decomposed to result in lower nitrogen content as featured by the ELNES.

Attempt has been made to measure the ELNES parameters in the $L_{2,3}$ edges of Ti and V. The absorption edge $L_{2,3}$ of transition metals consists of two sharp peaks originating from transitions from $2p^{1/2}$ and $2p^{3/2}$ initial states which have different energies. The structure of the $L_{2,3}$ absorption edge changes as the oxidation state varies, and changes from metallic state to oxide [11]. The double-peak structure of the Ti-$L_{2,3}$ and V-$L_{2,3}$ can be seen in Figures 5–7 and is illustrated in Figure 8. As the instrumental energy resolution was approximately 1.2 eV, which was too great to measure small differences in ELNES of the nitrides and the wear products, individual peak widths or positions could not be used to determine differences in structure of the tribofilm. For example, the TiAlN/VN V-$L_{2,3}$ edge exhibited full width at half maximum (FWHM) values of 3.0 eV for L_3 and 3.6 eV for L_2 respectively with a energy difference of 6.6 eV. However, by considering the whole $L_{2,3}$ edge as an single unit, a FWHM value of approximately 10–11 eV was obtained which is 10 times higher than the energy resolution. The $L_{2,3}$ FWHM values are shown in Figure 9, in which each error

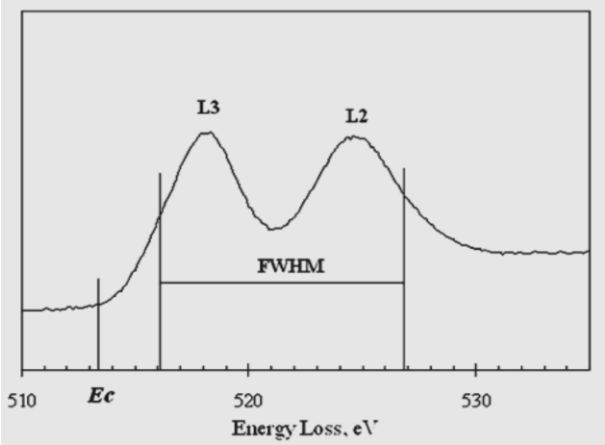

Figure 8. An V-L2,3 absorption edge of TiAlN/VN acquired at instrumental energy resolution 1.2 eV, energy dispersion of 0.1 eV/ pixal and local sample thickness t = 0.39k, to illustrate the measurement of ELNES peak parameter.

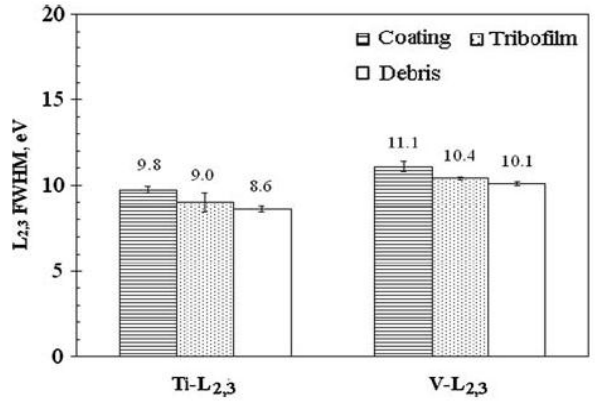

Figure 9. Comparison of the Ti- and V-L2,3 FWHM values between the nitride TiAlN/VN and the associated wear products. Note the decreased FWHM values in oxides (wear debris and tribofilm) as compared to the nitride.

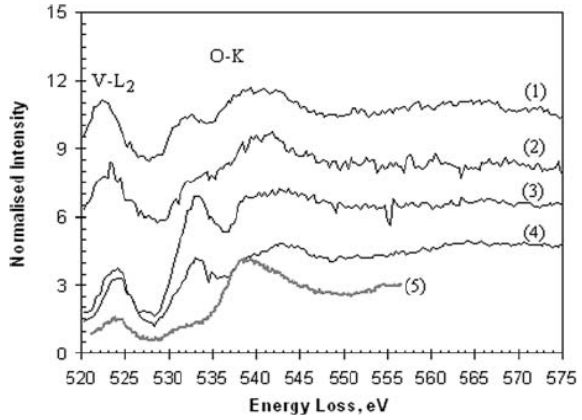

Figure 10. O-K absorption edges of (1–4) tribofilm and (5) wear debris.

bar was produced from at least three measurements. First, the FWHM values show a consistent decrease from nitride to oxide. The measurements confirmed the different chemical states of the TiAlN/VN coating prior to and after the tribo-oxidation. Secondly, the FWHM values of the tribofilm lie somewhere between those of the TiAlN/VN and wear debris and are closer to the latter. This was attributed to its domination of oxide and to the oxide-nitride co-existence.

Figure 10 shows a few typical EELS spectra of the tribofilm as compared to the spectrum of the wear debris. Each O-K absorption edge of the tribofilm contains two peaks in ranges 529–534.6 eV and 535.2–547.2 eV respectively and a much broader peak ranging from 558 to 596 eV. The

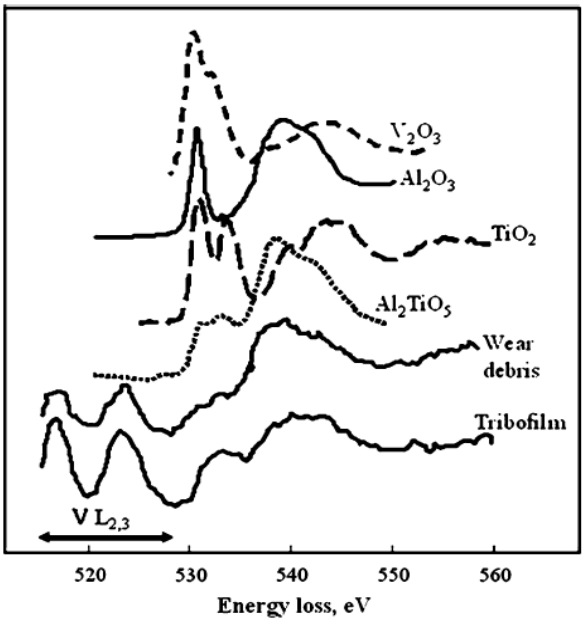

Figure 11. The O-K ELNES of tribofilm and wear debris as compared
to the ELNES patterns of other relevant oxides.

intensity of the first peak exhibited variation from area to area. In some areas, e.g. in spectrum (2), the intensity is so low that it become a shoulder in front of the second peak. On the other hand, the O-K edge of wear debris is clearly different from the tribofilm in that the shoulder intensity is even lower and the second peak is much stronger. Nevertheless, the ELNES comparison reveals structural and composition variation within the tribofilm. The variation in the O-K edge structure can be explained by the fact that the tribofilm was formed as a structurally inhomogeneous layer. This has been indicated in the TEM-EDX analysis where the spectra acquired in tribofilm regions exhibited lower intensity and larger variation from area to area compared to the adjacent nitride [25]. The structural inhomogeneity resulted from the dynamic sliding-mixing process and was also affected by the complex chemical and thermal interactions within the sliding contact zone.

As previous Raman spectroscopy of wear debris revealed weak presence of V_2O_5-like structure, further attempt was made to identify the oxide bonding structure by comparing the obtained O-K edge to those of known oxides, including V_2O_5 [20], Al_2O_3 [35], TiO_2 [36], and Al_2TiO_5 [35]. The comparisons are shown in Figure 11. $AlVO_4$ was excluded in the comparison because of the lack of relevant EELS data. The O-K edge shape of the binary oxides varies from V_2O_5, TiO_2 to Al_2O_3. None of them fits exactly to the shape of the O-K edge of tribofilm or wear debris. Thus, the wear product structure cannot be classified as any individual of the above oxides. This result can be explained by the fact that the tribofilm and wear debris analysed were in amorphous state and had multicomponent composition [25] whereas the sample spectra provided in literatures [20,35,36] were obtained in crystalline oxides with determined binary or ternary composition. In particular, it has been clarified that crystalline structured V_2O_5 oxide did not exist in the tribofilm. Then the only possible existence of V_2O_5-like structure, as revealed by the Raman spectroscopy result [19], would be in some short range ordered domains. Further analysis, e.g. the bonding structure at atomic scale, was beyond the available TEM instrumentation and the precision of sample preparation.

4. DISCUSSION

The innovative contribution of current experiments is the determination in nanometer scale of the chemical content and structure of the tribofilm and its parent base coating, which leads to deeper understanding on the tribo-oxidation mechanism of the TiAlN/VN and on the related friction and wear behaviour. A tribofilm can be generated on a solid surface experiencing dry sliding wear. This phenomenon has been found not only in TiAlN/VN, as presented in Figure 2 and more detailed in ref. [25,26], but also in other transition metal nitride coatings such as TiN, TiAlN/CrN and TiAlCrYN [28,30]. It has been shown that the tribofilm adhered on the TiAlN/VN surface with a distinct boundary was a densely packed agglomeration of oxide and nitride. The oxide was the predominant constitute, being in the form of an amorphous multicomponent Ti–Al–V–O mixture (Figures 2, 3, 5). The nitride was depleting in nitrogen as compared to the stoichiometric TiAlN/VN (Figure 5), evidencing a decomposition process of nitride debris within the tribofilm. The TiAlN/VN base coating adjacent to the tribofilm still retained its stoichiometric composition and structure and were free from oxygen.

The results presented suggest that oxidation of the TiAlN/VN under the dry sliding condition occurred mainly within the tribofilm through progressive decomposition of nitride debris. In a dry sliding process, wear debris may be generated during the initial stage of sliding wear through abrasion, edge cracking and adhesive breaking of asperity contacts between two rough surfaces [2,5]. In TiAlN/VN, it has been observed by high-resolution scanning electron microscopy that initial breaking of surface defect grains, i.e. the defects induced by lateral coating growth upon carthodic arc droplets, occurred as early as in the first 10–20 laps of sliding.More details of the observation will be published elsewhere. The debris were engaged within the sliding contact zone, which in one hand resulted in high-stress abrasive wear of the sliding surfaces and in other hand were expected to experience a process of breaking, refining and amorphorization. The latter led eventually to a densely packed agglomerate of debris adhered to the base TiAlN/VN surface. In ambient condition, oxygen and other oxidative species such as water vapour would unavoidably absorb on the debris surface. Additionally, sliding induced frictional heat causes substantially high flash temperature in the real asperity contacts [6]. The high flash temperature reached within the small asperity contact areas activates chemical reactions with the absorbed oxygen, leading to oxidation [1,2].

The oxidation process occurred in the sliding wear differs from the iso-thermal oxidation of TiAlN/VN and other nitrides. It is known that iso-thermal oxidation of nitrides occurs at elevated temperatures [15,19–21], so-called the onset oxidation temperature depending on the composition and structure of the nitrides. A metallographic feature of the diffusion-controlled iso-thermal oxidation is the existence of an intermediate or transition layer between the regions of un-oxidized nitride and newly formed oxide, which has been observed by using cross-sectional TEM, e.g. in [20]. In the case of tribooxidation, however, such transition zone does not exist, seeing Figure 2 and literatures [25,26,28,30].

The formation of tribofilm has significant influence on the friction and wear behaviour of TiAlN/VN and other hard coatings. It was reported in previous publication that several transition

metal nitride coatings, including TiAlN/VN, TiAlN/CrN, TiAlCrN and TiAlCrYN, showed coefficients of friction being as low as 0.2–0.3 irrelevant to the nitride composition and as high as 0.4–0.8 strongly depending on the chemical composition [14]. The increase in friction originated from the mechanical resistance in the wear product, i.e. breaking, refining and deformation of wear debris. The low-friction coefficient of TiAlN/VN is attributed to its vanadium-containing composition. Due to the lower shear strength of V_2O_5 oxide than other oxides, the V–O containing tribofilm exhibited lower friction coefficient. Similar low friction has been found in binary VN coatings [37] where TiAlN, another constituent subphase in the TiAlN/VN, generally exhibits high friction [13,14]. The extremely low wear coefficient of TiAlN/VN can be explained in three aspects. First, the low friction in dry sliding wear leads to low tangential load on the worn surface, therefore low severity of mechanical wear, and by decreasing the flash temperature which again decreases with decreasing friction [2,4], slows the oxidation rate. Secondly, the existence of a tribofilm reduces the severity of stress concentration by redistributes the sliding contact stresses. Thirdly, the TiAlN/VN multilayer itself possess superhardness in a range of 30–50 GPa as compared to its constituting nitrides TiAlN and VN in which the hardness values are usually less than 20 GPa [13,14,18,21]. High hardness in the superlattice multilayer nitrides provides further resistance against worn surface deformation and delamination wear [27,28].

5. CONCLUSIONS

A nanometer scale tribofilm formed on the worn surface of TiAlN/VN multilayer coating has been comprehensively characterized by using cross-section TEM and EELS analysis. The 20–50 nm thick amorphous-structured tribofilm exhibits a multicomponent V–Ti–Al–O–N composition with more pronounced oxygen content than nitrogen. Careful inspection of the ELNES features of the N-K as well as the Ti-$L_{2,3}$ and V-$L_{2,3}$ edges indicates decomposition of nitride debris in the tribofilm which dominated the tribo-oxidation. The loose wear debris is almost nitrogen-free and predominantly oxides indicating completion of the nitride decomposition. On the other hand, a sharp boundary was found to exist between the tribofilm and its base nitride coating. Along the boundary, neither inward diffusion of oxygen nor an oxygen-containing transition zone was found. This clearly indicates that, the tribooxidation was different from the diffusion-controlled iso-thermal oxidation of most nitride.

REFERENCES

[1] T.E. Fischer and W.M. Mullins, J. Phys. Chem. 96 (1992) 5690.
[2] S.K. Biswas, Wear 245 (2000) 178.
[3] W.M. Rainforth, A.J. Leonard, C. Perrin, A. Bedolla-Jacuinde, Y. Wang, H. Jones and Q. Luo, Tribol. Int. 35 (2002) 731.
[4] T.E. Fischer, Z. Zhu, H. Kim and D.S. Shin, Wear 245 (2000) 53.
[5] H. Engqvist, H. Hogberg, G.A. Botton, S. Ederyd and N. Axen, Wear 239 (2000) 219.
[6] M. Kalin and J. Vizintin, Tribol. Int. 34 (2001) 831.

[7] A. Blomberg, S. Hogmark and J. Lu, Tribol. Int.26 (1993) 369.
[8] S. Ruppi and M. Halvarsson, Thin Solid Films 353 (1999) 182.
[9] J.C. Sanchez-Lopez, C. Donnet, M. Belin, T. Le Mogne, C. Fernandez-Ramos, M.J. Sayagues and A. Fernandez, Surf. Coat. Technol. 133 (2000) 430.
[10] J.C. Sanchez-Lopez, A. Erdemir, C. Donnet and T.C. Rojas, Surf. Coat. Technol. 444 (2003) 163.
[11] W. Sigle, Ann. Rev. Mater. Res. 35 (2005) 239.
[12] I.M. Ross, W.M. Rainforth, A.J. Scott, A.P. Brown, R. Brydson and D.W. McComb, J. Eur. Ceram. Soc. 24 (2004) 2023.
[13] W.D. Münz, L.A. Donohue and P.Eh. Hovsepian, Surf. Coat. Technol. 125 (2000) 269.
[14] P.Eh. Hovsepian, D.B. Lewis and W.D. Münz, Surf. Coat. Technol. 166 (2000) 133.
[15] D.B. Lewis, S. Creasey, Z. Zhou, J.I. Forsyth, A.P. Ehiasarian, P.Eh. Hovsepian, Q. Luo, W.M. Rainforth and W.D. Münz, Surf. Coat. Technol. 177 (2004) 252.
[16] Q. Luo, P.Eh. Hovsepian, D.B. Lewis, W.D. Münz, Y.N. Kok, J. Cockrem, M. Bolton and A. Farinotti, Surf. Coat. Technol. 193 (2005) 39.
[17] Q. Luo, G. Robinson, M. Pittman, M. Howarth, W.-M. Sim, M.R. Stalley, H. R. Leitner Ebner, D. Caliskanoglu and P.Eh. Hovsepian, Surf. Coat. Technol. 200 (2005) 123.
[18] P.Eh. Hovsepian, Q. Luo, G. Robinson, M. Pittman, M. Howarth, D. Doerwald, R. Tietema, W.M. Sim and M.R. Stalley, Surf. Coat. Technol. 201 (2006) 265.
[19] C.P. Constable, J. Yarwood, P.Eh. Hovsepian, L.A. Donohue, D.B. Lewis and W.-D. Münz, J. Vac. Sci. Technol. A18 (2000) 1681.
[20] Z. Zhou, W.M. Rainforth, D.B. Lewis, S. Creasey, J.J. Forsyth, F. Clegg, A.P. Ehiasarian, P.Eh. Hovsepian and W.D. Münz, Surf. Coat. Technol. 198 (2004) 177.
[21] P.H. Mayrhofer, P.Eh. Hovsepian and W.D. Mitterer, Surf. Coat. Technol. 341 (2004) 177.
[22] D.S. Su, C. Hebert, H. Willinger and R. Schlogl, Micron 34 (2003) 227.
[23] A. Erdemir, Tribol. Lett. 8 (2000) 97.
[24] P.Eh. Hovsepian, D.B. Lewis, Q. Luo, W.-D. Münz, P.H. Mayrhofer, C. Mitterer, Z. Zhou and W.M. Rainforth, Thin Solid Films 485 (2005) 160.
[25] Q. Luo and P.Eh. Hovsepian, Thin Solid Films 497 (2006) 203.
[26] Z. Zhou, C.C. Calvert, Q. Luo, W.M. Rainforth, L. Chen and P.Eh. Hovsepian, J. Phys. Conf. Ser. 26 (2006) 95.
[27] Q. Luo, W.M. Rainforth and W.-D. Münz, Wear 74 (1999) 225.
[28] Q. Luo, W.M. Rainforth and W.-D. Münz, Scripta Mater 45 (2001) 399.
[29] D.B. Williams and C.B. Carter, Transmission Electron Microscopy IV: Spectrosmetry (Plenum Press, New York, 1996) 679.
[30] Q. Luo, Z. Zhou, W.M. Rainforth and P.Eh. Hovsepian, Surf. Coat. Technol., in press (2006).
[31] F. Hofer, P. Warbichler, A. Scott, R. Brydson, I. Galesic B. Kolbesen, J. Microscopy 204 (2001) 166.
[32] C. Mitterbauer, C. Hebert, G. Kothleitner, F. Hofer, P. Schattschneider and H.W. Zandbergen, Solid State Commun. 130 (2004) 209.
[33] M. MacKenzie, A.J. Craven and C.L. Collins, Scripta Mater 54 (2006) 1.
[34] L.A. Donohue, W.-D. Münz, D.B. Lewis, J. Cawley, T. Hurkmans, T. Trinh, I Petrov and JE Greene, Surf. Coat. Technol. 93 (1997) 69.
[35] D. Bouchet and C. Coliex, Ultramicroscopy 96 (2003) 139.
[36] C. Mitterbauera, G. Kothleitnera, W. Groggera, H. Zandbergenb, B. Freitagc, P. Tiemeijerc and F. Hofera, Ultramicroscopy 96 (2003) 469.
[37] G. Gassner, P.H. Mayrhofer, K. Kutschej, C. Mitterer and M. Kathrein, Tribol. Lett. 17 (2004) 751.